Model predictive control using Euler method for switched-battery boost-multilevel inverter

Ahmad Takiyuddin Abdullah[1,2], Sevia Mahdaliza Idrus[1], Shahrin Md Ayob[1]
[1]School of Electrical Engineering, Faculty of Engineering, Universiti Teknologi Malaysia, Johor, Malaysia
[2]Industrial Automation Section, UniKL MFI, Universiti Kuala Lumpur, Selangor, Malaysia

Article Info	ABSTRACT
	This paper presents the model predictive control (MPC) design using the backward Euler method for an 11-level switched-battery boost multilevel inverter (SBBMLI). The SBBMLI was proposed as the cost-effective solution for the communication power line in a high-speed rail (HSR) system. Initially, a generalized SBBMLI problem formulation was performed, and an open-loop simulation based on voltage and current mode controls was conducted. The finite control set-model predictive control (FCS-MPC) ability to track the reference sinusoidal output with low total harmonic distortion (THD) was then assessed as a performance criterion. Furthermore, the performance was assessed based on no-load and load disturbances. Finally, the results proved the ability of the proposed FCS-MPC to address non-linear dynamics, constraints, and its efficiency of implementation.

Corresponding Author:

Sevia Mahdaliza Idrus
School of Electrical Engineering, Faculty of Engineering, Universiti Teknologi Malaysia
Johor Bahru, Johor, Malaysia
Email: sevia@utm.my

1. INTRODUCTION

The work undertaken in this project unlocked a potent hardware-software fusion that can effectively solve the urgent requirements for the communication power line system in a high-speed rail (HSR) system. This can be accomplished by establishing control structures that can be applied to a newly developed inverter architecture with fewer components. Although the topology provides a number of advantages over traditional design, its full potential has not yet been explored.

Technology development for electrified railway networks has been heavily funded over the recent decades. The development does not involve the electric train but also systems within the train for traction, regenerative braking, and special power electronics applications [1]. These items additionally include numerous power electronics converter-based solutions.

Power electronics has proven to be essential technology in various fields that can convert electrical power from one form to another with high accuracy and efficacy for decades [2], [3]. Power inverters are essential for combining distributed generation sources (wind generator, photovoltaic) and energy storage systems into a micro-grid, which can supply local loads as well as link to the utility grid [4]. The importance of these converters such as in electrified trains is shown by the fact that they can be deployed in places other than within the train to improve power quality. They can also operate as a circuit interface between the high voltage three-phase power grid and the medium voltage single-phase traction power grid [1]. The use of inverters, also known as dc-ac converters, can be found in medium- or high-power systems, such as static reactive power compensation and adjustable-speed drives, and has unquestionably made a substantial

contribution. Yet, new multilevel inverter circuit concepts have advanced due to significant electromagnetic interference (EMI) difficulties and stress across the power switches. Being based on low-frequency switching and allowing for voltage and current sharing across the power semiconductors, the multilevel notion is often a fresh solution in these applications [5], [6]

The MLI is currently acknowledged as cutting-edge technology for converting dc to ac power in the sectors of generation, transmission, distribution, and use [7]. The most common multilevel inverter topologies are diode-clamped (neutral-point clamped), capacitor-clamped (flying capacitor), and cascaded H-bridge [8]. The cascaded H-Bridge is regarded as popular and well-accepted by industries with its modular structure, simple to control, and not having an imbalance capacitor voltage problem as the neutral-point clamp inverter. However, the limitation of the cascaded H-bridge is that it requires separate dc sources. The number of components, especially the power switches, is considerably higher compared to the such as neutral-point clamp inverter. On the other hand, the emerge of transformer less inverters have grown significantly in popularity due to their desirable qualities, such as higher efficiency, smaller size, lower cost, and higher power density. These inverters are particularly well suited for small-scale grid-connected PV systems [9]–[10]. The biggest issue with these inverters, though, is the leakage current. As a result, it becomes more important to use specific inverter topologies and dedicated switching approaches [9], [11], [12], which reduces efficiency and increases control complexity.

In order to address the aforementioned problems, this research employs an architecture called as a switched-battery boost-multilevel inverter (SBBMLI) [7]. Comparatively speaking, it requires a lot fewer power switches than a cascaded H-bridge multilevel inverter. This architecture will result in a smaller system, which will lower costs and enhance dependability. The goal is to create innovative, cost-effective solutions for integrating renewable energy sources into the grid, such solar power. The ability of the inverter to operate a single PV module for a 1 kW prototype is another crucial requirement. The outcome should also be taken into account for the recommended attributes of its dependability, surge power capability and efficiency [8]. The low-order harmonics will be eliminated and the desired fundamental components will be controlled, using an efficient control approach. The management of the charging mode, inverter mode, and battery will also be performed via an effective control scheme. Although there are numerous other control schemes that can be employed [13], the model predictive control (MPC) scheme is widely used to achieve the goal of the aforementioned type. The MPC is chosen since it has demonstrated its applicability to regulate power converters such that the ideas are clear and understandable. It applies to several systems, constraints, and nonlinearities that are simple to include. The multivariable scenario can be considered, and the resulting controller is simple [14].

The three-level NPC inverter at the grid side has been applied to the backward Euler method approach of MPC. It manages the reactive power to the grid and net dc-bus voltage in a medium-voltage wind energy conversion system. The application of an FCS-MPC approach has led to the achievement of a rapid dynamic response. There was no longer any use of linear controllers or modulation stages [15]. An adaptive observer-based MPC has been used to regulate a multilayer flying capacitor inverter in another typical topology. Theoretical analysis and experimental findings in this instance demonstrate that the suggested strategy is effective even in the existence of disturbances, such as load change, input change, and parameter variations, and is stable for all system configurations [16]. Using the Euler method, the MPC has also been implemented on a multilevel cascaded H-bridge. This MPC approach selected the voltage vector that minimized a cost function to project the future value of the current for all voltage vectors using a discrete-time model of the system. The work has been claimed to perform well in terms of reference tracking and reduced common-mode voltages because of the implementation of a rapid calculation algorithm [17]. Another control strategy has also been developed using the MPC framework and the Euler method. The MPC predicts the states of a single-phase dual-mode inverter with an MPC algorithm. By proposing an auto-tuning strategy for the MPC cost function, the weight factor tuning strategy was made simpler. The results show that the load voltage is regulated without interruption and distortion [18].

Conventional topology has also been developed to reduce the components of a multilevel inverter. A reduced multilevel converter was acquired using the MPC technique. Its main idea is that the basic dc cell, which is able to provide the variable dc-link voltage, has a regulated approach through the floating capacitors. This feature offers the output phases of the converter with the degree of control necessary to enable a shared multilevel dc-link. When this converter topology was investigated using FCS-MPC, the results showed that dc-cell capacitors could be balanced and accurately controlled to achieve sinusoidal output currents and a five-level output voltage waveform [19].

In controlling the flow of electrical energy using power converters, which includes the subcategory of inverters, MPC has been proven to give a highly straightforward and efficient alternative to traditional control algorithms utilizing pulse width modulation (PWM) [14], [20], [21]. Moreover, the predictive

technique has the ability to adjust current, voltage, torque, flux, and other factors by developing an appropriate cost function [22].

The analysis presented above demonstrates the effective use of MPC for inverters employing controllers adapted to certain topologies. The basic principle of FCS-MPC is to anticipate the system's behavior in response to a finite set of potential control actions using a discrete model of the system. This enables it to directly select the best actuation based on an optimization criterion [23]. However, a major shortcoming of the FCS-MPC is its computational burden, which increases with the number of switching states [24]. Because the SBBMLI has provided fewer switching states, extra consideration must be given to decreasing computational load while applying FCS-MPC to a multilevel inverter that satisfies its topology.

2. MPC CONTROL DESIGN USING EULER METHOD

The underpinning of MPC is a dynamic model of the process, frequently a linear empirical model created by system identification. The primary innovation of MPC is that it optimizes the input at the present time while taking into consideration potential future inputs. Over a finite-time horizon, it is achieved by repeatedly optimizing the control output through the current input value. Correspondingly, MPC can anticipate future events and can take control actions accordingly. This unique feature differentiates the MPC from the linear-quadratic regulator (LQR). Though research is being done to find a faster response time with specifically built analog circuitry, the MPC is typically implemented as digital control [25].

In the case of robust variants relevant to industrial applications, MPC can consider set bounded disturbances while still ensuring state constraints are met. In general, the basic components of MPC are as follows [26]–[27]:

− Mathematical model of the controlled plant to calculate the evolution of the system states over time.
− Optimal control problem: The changes of the control variables are described by a system of differential equations termed optimal control that minimizes the cost function. The control objectives are stated as an objective function. When the optimization issue is resolved, the best control strategy for the plant's best performance over the forecast horizon is derived. It should be emphasized that the prediction horizon refers to the period of time during which the control measures are prepared and the plant's behavior is predicted.
− Receding horizon policy: The remaining components are eliminated under the receding horizon strategy, the prediction horizon is advanced by one sample instant, and the optimization process is resumed, only implementing the first component in the optimal sequence of the control inputs to the plant.

Future response in the mathematical model of a regulated plant is predicted using a dynamic model. The following defines the state-space representation for discrete-time linear systems:

$$x(k + 1) = Ax(t) + Bu(k) \tag{1}$$

where at the kth sampling instant, $x(k)$ and $u(k)$ are the model state and input vectors. A predicted input sequence is used to generate the corresponding series of state predictions by simulating the model forward over the prediction horizon, assuming N-sampling intervals. Frequently, these predicted sequences are stacked into the vectors u, x, which are defined as follows:

$$u = \begin{bmatrix} u(k|k) \\ u(k+1|k) \\ \vdots \\ u(k+N-1|k) \end{bmatrix} x = \begin{bmatrix} x(k|k) \\ x(k+1|k) \\ \vdots \\ x(k+N-1|k) \end{bmatrix} \tag{2}$$

In this instance, $x(k + i|k)$ evolves in accordance with the prediction model because the input and state vectors at time $k + i$ that are predicted at time k are denoted by $u(k + i|k)$ and $x(k + i|k)$:

$$x(k) = Ax(k) + Bu(k), i = 0, 1, \dots \tag{3}$$

where the initial condition of the prediction horizon is defined as:

$$x(k) = x(k) \tag{4}$$

As a result of computing the predicted sequences u, x for the predictive control feedback rule, the optimal control problem minimizes a predicted performance cost. An anticipated cost in the case of quadratic cost is defined as having the general form:

$$J(k) = \sum_{i=0}^{N}[x^T(k+i|k)Qx(k+i|k) + u^T(k+i|k)Ru(k+i|k)] \tag{5}$$

where N is sampling intervals and Q, R are positive definite matrices (Q may be positive semi-definite). The optimal input sequence for the issue of minimizing $J(k)$ is designated u*(k) and is defined as (6).

$$u^*(k) = arg\ \min_{u} J(k) \tag{6}$$

If the plant is subject to input and state constraints, the optimization might be incorporated as equivalent constraints on u*(k).

A general-purpose control scheme that upcoming repeatedly solving a constrained optimization problem and selecting the control action according to predictions of upcoming costs, disturbances, and constraints over a moving temporal horizon is known as receding horizon control. Input to the plant is only the first element of the optimal predicted input sequence u*(k), which is described as (7).

$$u(k) = u^*(k|k) \tag{7}$$

At each sampling instant where $k = 0, 1, ...,$ the procedure of determining u*(k) by minimizing the predicted cost and implementing the first element of u is repeated. Therefore, the optimization defining u* is known as online optimization. Figure 1 shows the receding horizon strategy, in which the prediction horizon has remained constant in length despite optimization at subsequent instants.
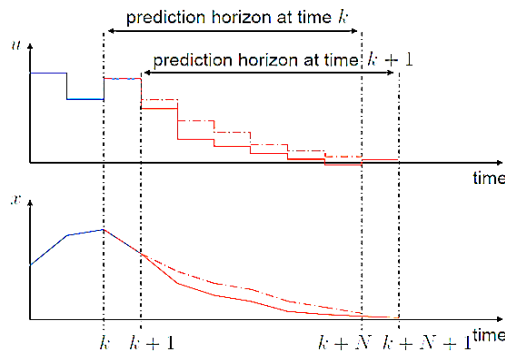

Figure 1. The receding horizon strategy

Since the state predictions x and, subsequently, the optimal input sequence u* depend on the current state measurement $x(k)$, the approach incorporates feedback into the MPC rule, offering a degree of robustness to modelling errors and uncertainty. The receding horizon technique likewise attempts to take into consideration the finite horizon by continually adjusting the horizon across which future inputs are optimized. The initial step in applying advanced MPC to the SBBMLI topology is to use the existing MPC implementation method on a conventional topology. Figure 2 shows the MPC design using the Euler backward method for the SBBMLI.

The employed MPC controller embeds a discrete-time model for the prediction of control variables of current and voltage at a certain sampling time, T_s. The T_s is set at $25\ \mu s$ for all simulation involved. Because power converters are discrete devices, an online implementation of the optimization issue is now feasible. The online evaluation of each switching state permits the choice of the best actuation under the constraints of a finite number of switching states and the present generation of microprocessors. This approach is referred to as a finite control set MPC because the switching states of power converters give rise to a finite number of available actions.

Based on the literature review, the Euler method is commonly utilized to produce a discrete-time model. The following are the design steps of MPC's finite control set for controlling a power converter:
− Modelling the system by identifying all potential switching states and the relationships between the input and output.
− Establishing a cost function to describe the desired action, such as tracking the reference to a suitable system variable.
− Acquiring discrete-time models that allow for the future behavior of the controllable variables to be predicted.
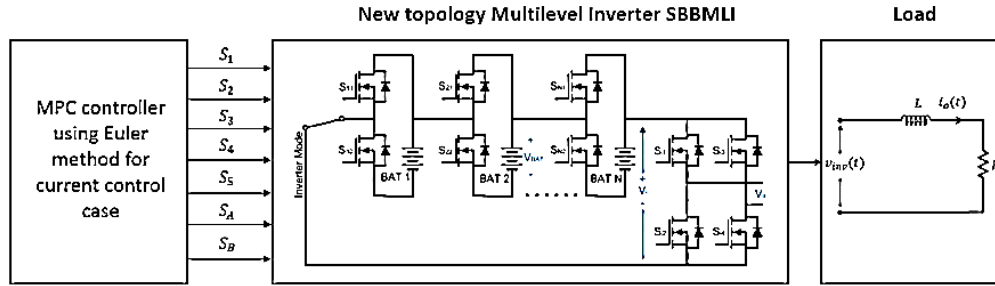
Figure 2. MPC using Euler method for current control implementation

By considering the ideal switch of a power transistor, the simplest model can be realized by the states of "on" (1) and "off" (0). In this case, a general rule for the number of possible switching states, N, with the exception of specific combinations, such as the combination that short-circuits the dc link, is as:

$$N = x^y \tag{8}$$

where y is the number of converter legs and x is the number of potential states for each converter leg.

The prediction model must consider the controlled variables to derive discrete-time models that can predict these variables. In addition, defining the measured and unmeasured variables is also important since the predictive model needs estimation for the unmeasured variable. Finally, the discretization method is applied to yield the discrete-time model. For example, in a first-order system, the Euler forward method is used to approximate the derivative as described below, as used in [22]:

$$\frac{dx}{dt} = \frac{x(k+1) - x(k)}{T_s} \tag{9}$$

where T_s is the sampling time.

The cost function relates to the specific application being considered upon. Each application employs the most appropriate cost function to specify the desired behavior of the state variables of interest. Several terms related to the tracking error of these state variables compose up the cost function. To control them simultaneously, only one cost function is necessitated [28]. The cost function for the current control is described as:

$$g = |i^* - i_o(k+1)| \tag{10}$$

where the reference current vector and predicted voltage vector are denoted as i^* and $i_0(k+1)$ respectively.

The following is a description of the discrete-time model for the load current prediction:

$$i_o(k+1) = i(k)\left(1 - \frac{RT_s}{L}\right) + \frac{T_s}{L} v_{inv}(k) \tag{11}$$

where R is resistance load and L is inductance load, T_s is the sampling time, $i(k)$ is the measured load current and $i_o(k+1)$ is the predicted current to be considered in the controller optimization.

The similar concept to the Euler Method is designed for voltage control by applying MPC. Figure 3 shows the considered MPC scheme using the Euler method for voltage control implementation on SBBMLI. The voltage control has been selected because it matches the needs of the MPC application.

The discrete-time model for the prediction of the load voltage is described as:

$$g = |v^* - v_o(k+1)|^2 \tag{12}$$

where v^* is the reference voltage vector and $v_o(k+1)$ is the predicted voltage vector:

$$v_o(k+1) = \frac{CL}{CL + T_s^2}\left\{v_o(k) + \frac{T_s}{C}[i_L(k) - i_o(k+1)] + \frac{T_s^2}{C} v_{inv}(k+1)\right\} \tag{13}$$

where C is the capacitance load and L is inductance load, T_s is the sampling time, $v_o(k)$ is the measured load voltage, $i_o(k) \approx i_o(k+1)$ when T_s is small and $v_o(k+1)$ is predicted voltage to be considered in the

controller optimization. The MPC algorithm flowchart for the current control of 11-level SBBMLI is shown in Figure 4(a), whereas, the voltage control of 11-level SBBMLI is shown in Figure 4(b).
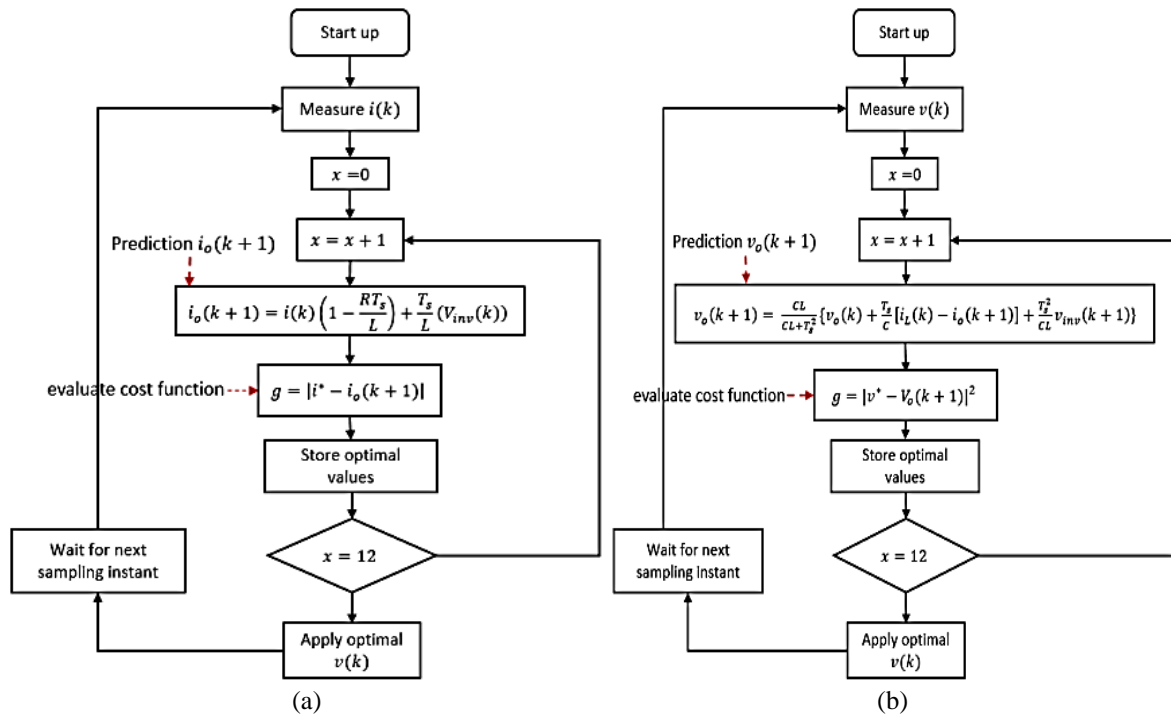

Figure 4: The MPC algorithm flowchart for current control and voltage control of 11-level SBBMLI: (a) current control and (b) voltage control

3. RESULTS AND DISCUSSION

There are numerous switch combinations that might be built to generate an 11-level output voltage. Nevertheless, Table 1 lists one possible combination of the switching states of the 11-level SBBMLI. The simulation has been conducted under both current control and voltage control. The output load comprises a resistor (R = 10 Ω) and the inductor (L = 10 mH) for the current control configuration without the LC filter before the load. Figure 5 shows the I_{ref} and Io of MPC current control. It shows accurate tracking behavior of I_o with a small error compared to I_{ref}. The FFT analysis of the total harmonic distortion (THD) is presented in Figure 6. The MPC has given rise to a small value of 1.24% THD.
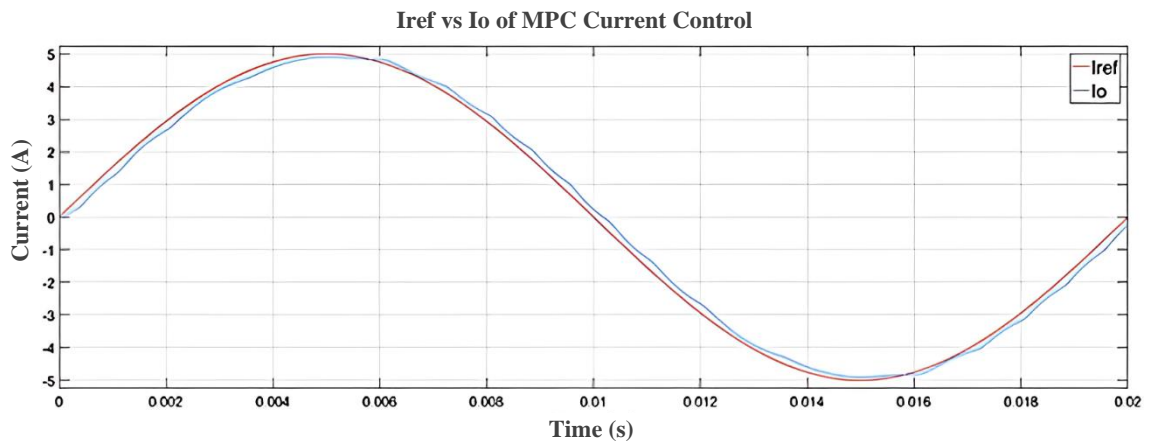
Figure 5. I_{ref} and I_o of MPC current control
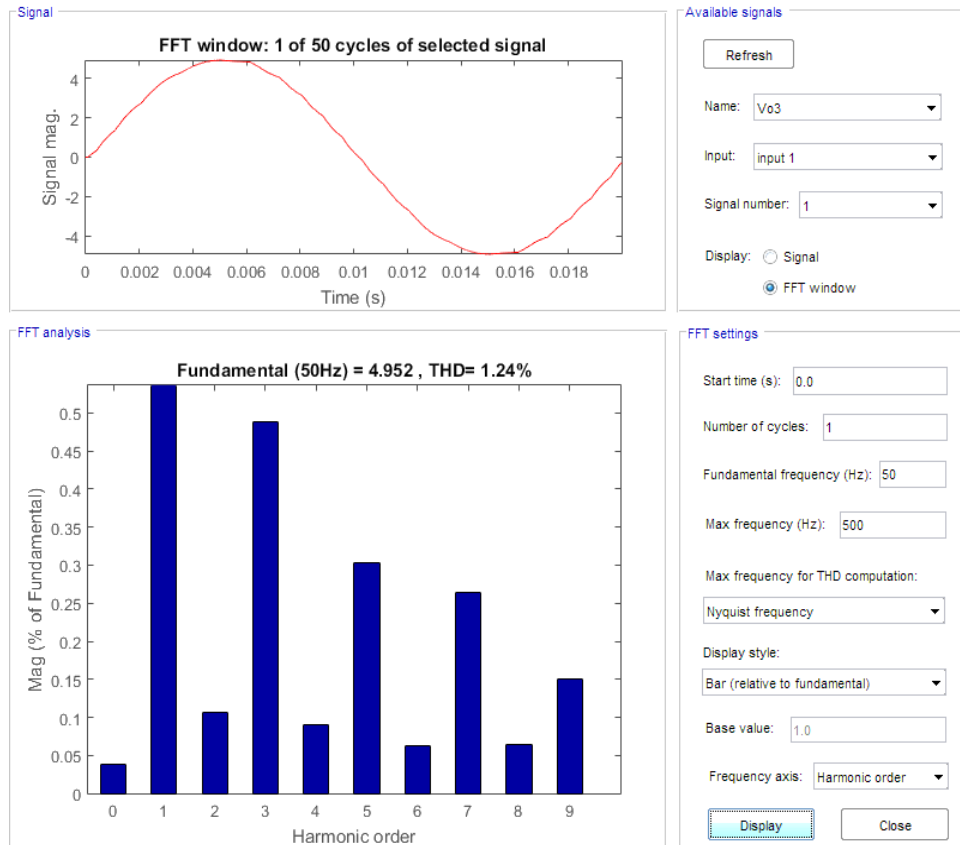
Figure 6. The FFT analysis of THD for current control configuration

Table 1. The switching states for the simulation of 11-level SBBMLI

Vector	$v_{inv}(k+1)$	S_1	S_2	S_3	S_4	S_5	S_A	S_B
V_0	0	0	0	0	0	0	0	0
V_1	Vdc	1	0	0	0	0	1	0
V_2	$2V_{dc}$	1	1	0	0	0	1	0
V_3	$3V_{dc}$	1	1	1	0	0	1	0
V_4	$4V_{dc}$	1	1	1	1	0	1	0
V_5	$5V_{dc}$	1	1	1	1	1	1	0
V_6	$-V_{dc}$	1	0	0	0	0	0	1
V_7	$-2V_{dc}$	1	1	0	0	0	0	1
V_8	$-3V_{dc}$	1	1	1	0	0	0	1
V_9	$-4V_{dc}$	1	1	1	1	0	0	1
V_{10}	$-5V_{dc}$	1	1	1	1	1	0	1
V_{11}	0	1	1	1	1	1	1	1

The simulation is then run under voltage control configuration with the inverter output comprising the LC filter (L = 2 mH and C = 2 µF) and load (R_l = 10 Ω). Figure 7 describes the reference V_{ref} and output voltage V_o. The result shows better tracking behavior of V_o with a very small error. The FFT analysis of the THD is depicted in Figure 8. The MPC has given rise to a very small value of 0.48% THD.

The results establish the feasibility of the initial MPC simulation using a receding horizon strategy. The converter is subsequently subjected to the switching state, which minimizes a cost function, after the evaluation of the predictions. One of the most crucial phases in the design of an MPC scheme is the cost function formulation since it enables the choice of the control objectives for the application and the inclusion of any necessary constraints.

A comparison of open-loop simulation and MPC using the Euler method (closed-loop simulation) on v_{inv}, v_o, i_L and i_o for the load without disturbance is shown in Figure 9. The results show more ripple, which means a greater error in the v_o, i_L and i_o open-loop signals compared to MPC. Figure 10 shows a comparison between open-loop simulation and MPC for v_o and i_o signals for the load with disturbance. The load with disturbance was also considered when the 10 Ω load is reduced to 5 Ω during the simulation. The

output voltage v_o for both configurations is apparent to be unaffected by the disturbance, except a spike at initial changes of load 5 Ω to 10 Ω. The result has also shown that the initial spike is less for MPC using the Euler method than an open loop. Figure 11 shows a comparison of THD (v_o) for open-loop in Figure 11(a) and MPC for the disturbance case in Figure 11(b). MPC increased THD by 0.56% compared to open-loop 2.03%. In the case of MPC for a load without disturbance, the THD value is 0.48%, as shown in Figure 8.
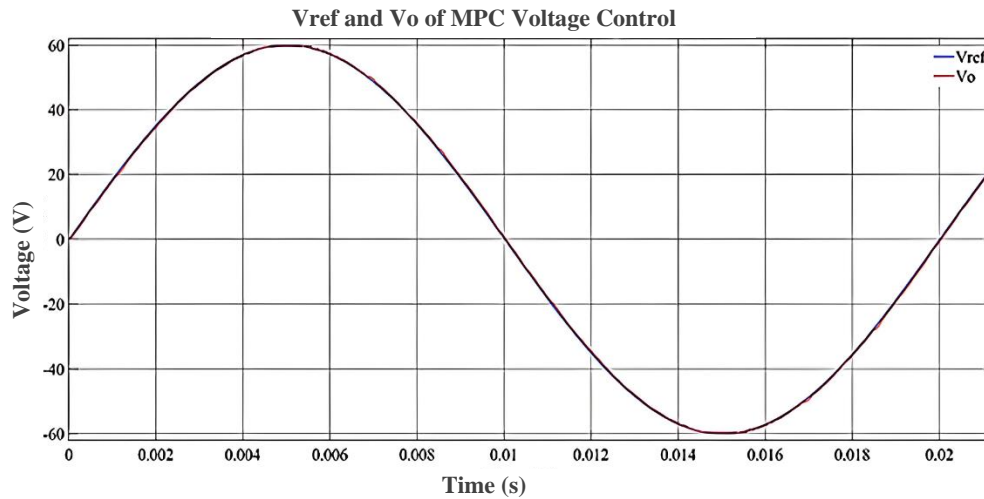
Figure 7. V_{ref} and V_o of MPC voltage control
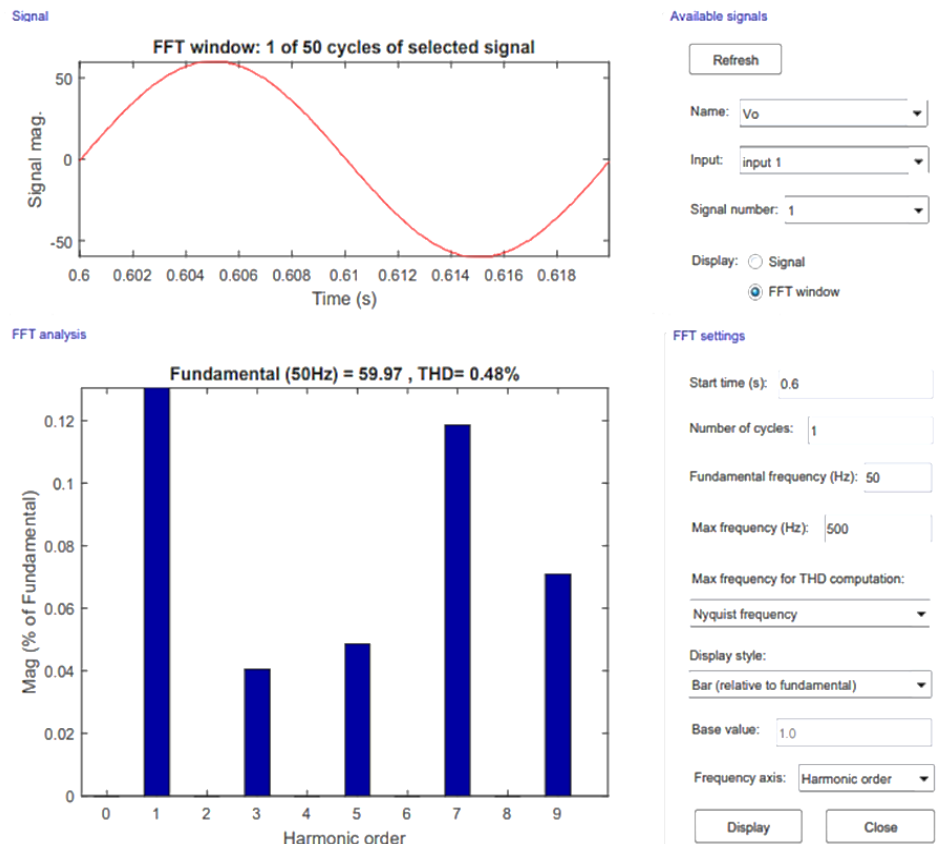
Figure 8. The FFT analysis of THD for voltage control configuration
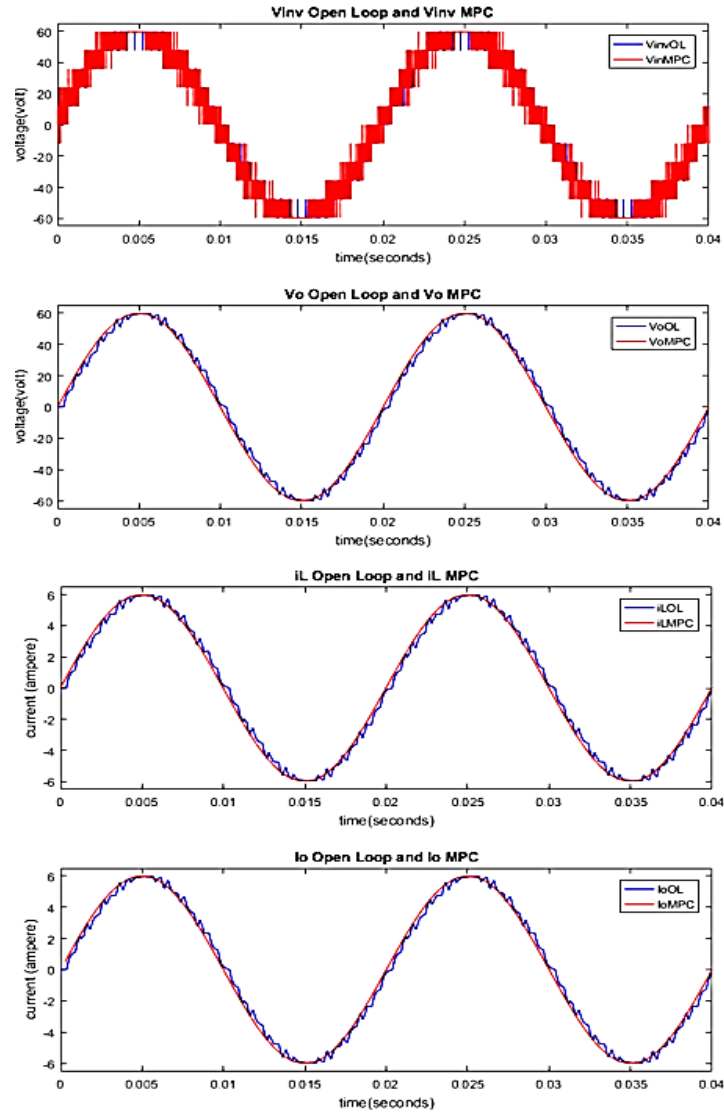
Figure 9. Comparison of open-loop and MPC for the configuration load without disturbance
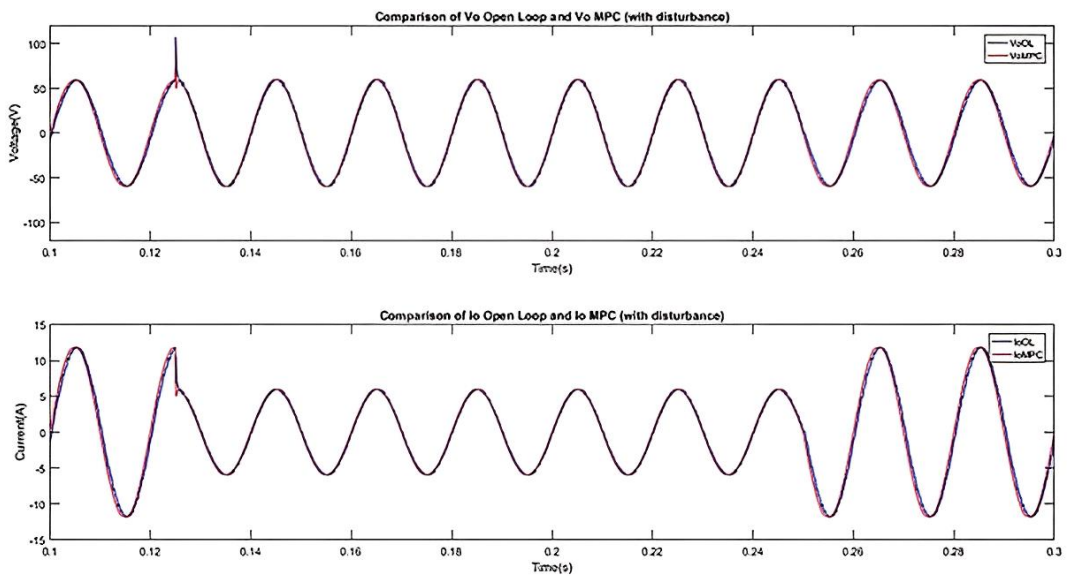
Figure 10. Comparison of I_o and V_o of open-loop and MPC for the configuration load with disturbance

(a)

(b)
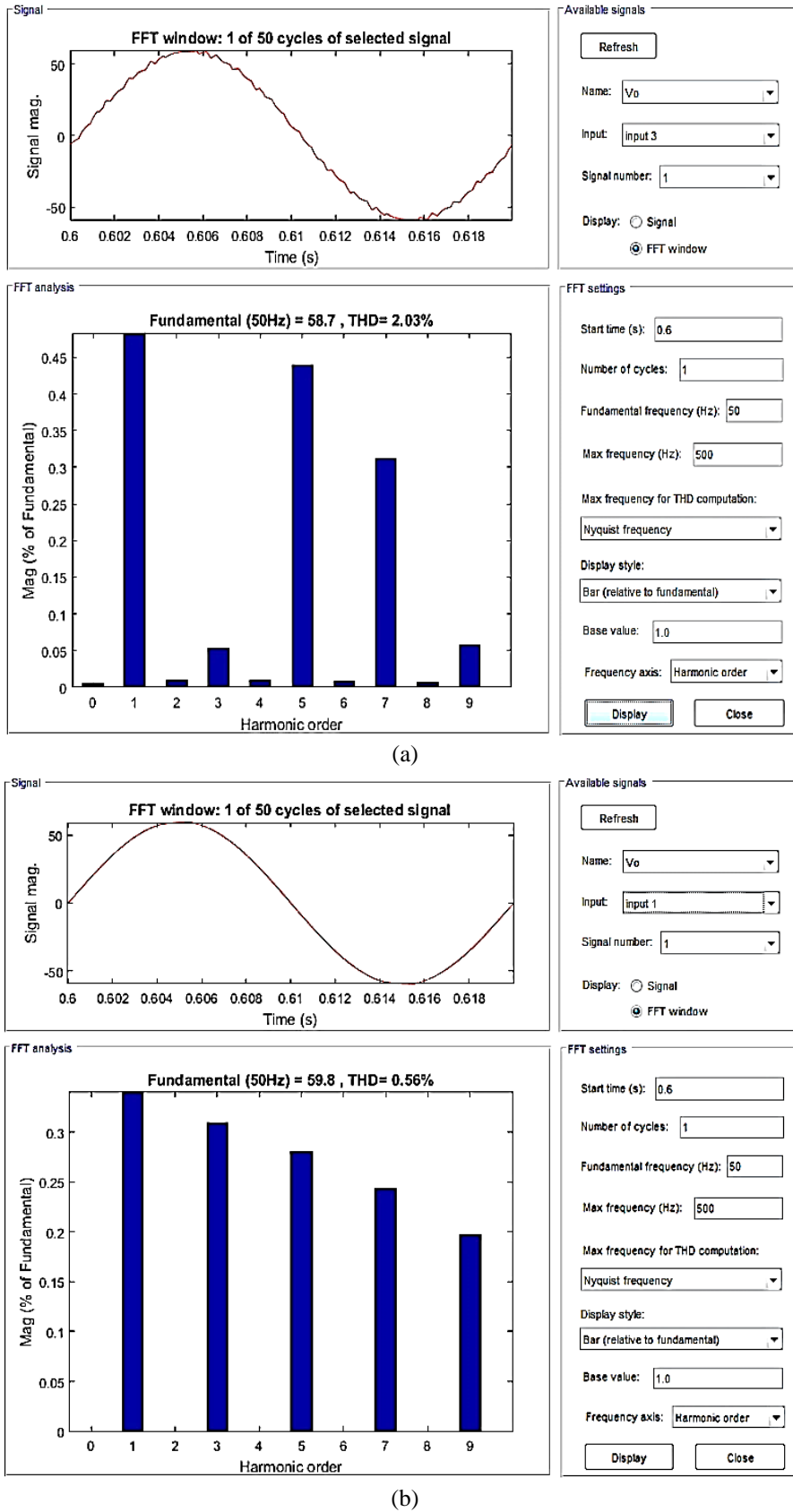
Figure 11. Comparison of THD (v_o) for open-loop and MPC for the configuration load with disturbance:
(a) THD open-loop and (b) THD MPC using Euler method

4. CONCLUSION

The results establish the feasibility of the initial MPC simulation using a receding horizon strategy. Determining the cost function is the most essential aspects in developing an MPC scheme since it enables the selection of the application's control objectives and the inclusion of any relevant constraints. Application of the switching state, which minimizes a cost function, to the converter is performed after evaluation of the predictions. Within the simulation executed on the SBBMLI, the MPC using the Euler method has given 1.24% and 0.48% of THD for current control and voltage control configurations, respectively. Furthermore, the THD with disturbance has increased to 0.56% by using the MPC compared to the open-loop, which has given 2.03%."

REFERENCES

[1] J. L. Afonso *et al.*, "A review on power electronics technologies for electric mobility," *Energies*, vol. 13, no. 23, 2020, doi: 10.3390/en13236343.

[2] N. Mohan, T. M. Undeland, and W. P. Robbins, *Power electronics : converters, applications, and design*. Hoboken, N.J. : Wiley, 2003.

[3] M. H. Rashid, *Power electronics: devices, circuits, and applications*. Pearson education, 2014.

[4] Y. Yang and R. J. Wai, "Design of Adaptive Fuzzy-Neural-Network-Imitating Sliding-Mode Control for Parallel-Inverter System in Islanded Micro-Grid," *IEEE Access*, vol. 9, pp. 56376–56396, 2021, doi: 10.1109/ACCESS.2021.3071832.

[5] G. S. Perantzakis, F. H. Xepapas, and S. N. Manias, "A Novel Four-Level Voltage Source Inverter;Influence of Switching Strategies on the Distribution of Power Losses," *IEEE Transactions on Power Electronics*, vol. 22, no. 1, pp. 149–159, Jan. 2007, doi: 10.1109/TPEL.2006.886627.

[6] Y. Cheng, C. Qian, M. L. Crow, S. Pekarek, and S. Atcitty, "A Comparison of Diode-Clamped and Cascaded Multilevel Converters for a (STATCOM) With Energy Storage," *IEEE Transactions on Industrial Electronics*, vol. 53, no. 5, pp. 1512–1521, Oct. 2006, doi: 10.1109/TIE.2006.882022.

[7] S. Choudhury, M. Bajaj, T. Dash, S. Kamel, and F. Jurado, "Multilevel inverter: A survey on classical and advanced topologies, control schemes, applications to power system and future prospects," *Energies*, vol. 14, no. 18, 2021, doi: 10.3390/en14185773.

[8] S. Daher, J. Schmid, and F. L. M. Antunes, "Multilevel inverter topologies for stand-alone (PV) systems," *Industrial Electronics, IEEE Transactions on*, vol. 55, no. 7, pp. 2703–2712, 2008.

[9] S. Kakar *et al.*, "A Common-Ground-Type Five-Level Inverter with Dynamic Voltage Boost," *Electronics (Switzerland)*, vol. 11, no. 24, pp. 1–10, 2022, doi: 10.3390/electronics11244174.

[10] U. Mustafa, M. S. Bin Arif, S. Md Ayob, and M. Tariq, "Single Phase Seven-Level Inverter topology with Single DC Source and Reduce Device Count for Medium and High Power Applications," *2019 Innovations in Power and Advanced Computing Technologies, i-PACT 2019*, pp. 1–6, 2019, doi: 10.1109/i-PACT44901.2019.8960170.

[11] X. Guo, R. He, J. Jian, Z. Lu, X. Sun, and J. M. Guerrero, "Leakage current elimination of four-leg inverter for transformerless three-phase PV systems," *IEEE Transactions on Power Electronics*, vol. 31, no. 3, pp. 1841–1846, 2016, doi: 10.1109/TPEL.2015.2477539.

[12] U. Mustafa, M. S. Bin Arif, S. Ahmad, M. Tariq, and S. M. Ayob, "Performance Evaluation of Modified 5-Level T-Type H-Bridge Inverter Utilizing Different PWM Modulation Schemes," *2019 Innovations in Power and Advanced Computing Technologies, i-PACT 2019*, pp. 1–6, 2019, doi: 10.1109/i-PACT44901.2019.8960095.

[13] A. Poorfakhraei, M. Narimani, and A. Emadi, "A Review of Modulation and Control Techniques for Multilevel Inverters in Traction Applications," *IEEE Access*, vol. 9, pp. 24187–24204, 2021, doi: 10.1109/ACCESS.2021.3056612.

[14] P. Cortes, M. P. Kazmierkowski, R. M. Kennel, D. E. Quevedo, and J. Rodriguez, "Predictive Control in Power Electronics and Drives," *IEEE Transactions on Industrial Electronics*, vol. 55, no. 12, pp. 4312–4324, Dec. 2008, doi: 10.1109/TIE.2008.2007480.

[15] V. Yaramasu and B. Wu, "Predictive Control of a Three-Level Boost Converter and an NPC Inverter for High-Power PMSG-Based Medium Voltage Wind Energy Conversion Systems," *IEEE Transactions on Power Electronics*, vol. 29, no. 10, pp. 5308–5322, Oct. 2014, doi: 10.1109/TPEL.2013.2292068.

[16] M. Ghanes, M. Trabelsi, H. Abu-Rub, and L. Ben-Brahim, "Robust Adaptive Observer-Based Model Predictive Control for Multilevel Flying Capacitors Inverter," *IEEE Transactions on Industrial Electronics*, vol. 63, no. 12, pp. 7876–7886, Dec. 2016, doi: 10.1109/TIE.2016.2606359.

[17] P. Cortes, A. Wilson, S. Kouro, J. Rodriguez, and H. Abu-Rub, "Model Predictive Control of Multilevel Cascaded H-Bridge Inverters," *IEEE Transactions on Industrial Electronics*, vol. 57, no. 8, pp. 2691–2699, Aug. 2010, doi: 10.1109/TIE.2010.2041733.

[18] X. Li, H. Zhang, M. B. Shadmand, and R. S. Balog, "Model Predictive Control of a Voltage-Source Inverter With Seamless Transition Between Islanded and Grid-Connected Operations," *IEEE Transactions on Industrial Electronics*, vol. 64, no. 10, pp. 7906–7918, Oct. 2017, doi: 10.1109/TIE.2017.2696459.

[19] M. Norambuena, S. Kouro, S. Dieckerhoff, and J. Rodriguez, "Reduced Multilevel Converter: A Novel Multilevel Converter With a Reduced Number of Active Switches," *IEEE Transactions on Industrial Electronics*, vol. 65, no. 5, pp. 3636–3645, May 2018, doi: 10.1109/TIE.2017.2762628.

[20] A. T. Abdullah, S. M. Idrus, and S. M. Ayob, "Performance Analysis of FCS-MPC Using the Generalized Formulation and Euler Method on SBBMLI," *5th IEEE Conference on Energy Conversion, CENCON 2021*, pp. 85–90, 2021, doi: 10.1109/CENCON51869.2021.9627244.

[21] S. Kouro, P. Cortes, R. Vargas, U. Ammann, and J. Rodriguez, "Model Predictive Control 2014;A Simple and Powerful Method to Control Power Converters," *IEEE Transactions on Industrial Electronics*, vol. 56, no. 6, pp. 1826–1838, Jun. 2009, doi: 10.1109/TIE.2008.2008349.

[22] J. Rodriguez and P. Cortes, *Predictive control of power converters and electrical drives*, vol. 40. John Wiley \& Sons, 2012.

[23] M. Aguirre, S. Kouro, C. A. Rojas, J. Rodriguez, and J. I. Leon, "Switching Frequency Regulation for FCS-MPC Based on a Period Control Approach," *IEEE Transactions on Industrial Electronics*, vol. 65, no. 7, pp. 5764–5773, 2018, doi: 10.1109/TIE.2017.2777385.

[24] S. R. Mohapatra and V. Agarwal, "Model Predictive Control for Flexible Reduction of Active Power Oscillation in Grid-Tied Multilevel Inverters under Unbalanced and Distorted Microgrid Conditions," *IEEE Transactions on Industry Applications*, vol. 56, no. 2, pp. 1107–1115, 2020, doi: 10.1109/TIA.2019.2957480.

[25] S. Vichik and F. Borrelli, "Solving linear and quadratic programs with an analog circuit," *Computers & Chemical Engineering*, vol. 70, pp. 160–171, 2014.

[26] E. F. Camacho and C. B. Alba, *Model predictive control*. Springer science & business media, 2013.

[27] P. Karamanakos and T. Geyer, "Guidelines for the Design of Finite Control Set Model Predictive Controllers," *IEEE Transactions on Power Electronics*, vol. 35, no. 7, pp. 7434–7450, 2020, doi: 10.1109/TPEL.2019.2954357.

[28] S. Vazquez, E. Zafra, R. P. Aguilera, T. Geyer, J. I. Leon, and L. G. Franquelo, "Prediction model with harmonic load current components for FCS-MPC of an uninterruptible power supply," *IEEE Transactions on Power Electronics*, vol. 37, no. 1, pp. 322–331, 2022, doi: 10.1109/TPEL.2021.3098948.

BIOGRAPHIES OF AUTHORS

Ahmad Takiyuddin Abdullah 🆔 is a PhD student in Faculty of Electrical Engineering, Universiti Teknologi Malaysia (UTM) since 2021. He has been a lecturer in Industrial Automation Section, Universiti Kuala Lumpur Malaysia France Institute since 2007. He received his B.Eng. in Electrical and Electronic Engineering from Liverpool John Moores University, United Kingdom in 1997. He obtained M.Eng. in Electrical (Mechatronics & Automatic Control) from UTM in 2006. His research interests include the field of control system, power electronics, robotics, signal processing and communication system. He can be contacted at email: ahmadtakiyuddin@graduate.utm.my.

Sevia Mahdaliza Idrus 🆔 received her Bachelor in Electrical Engineering in 1998 and Master in Engineering Management in 1999, both from UTM. She obtained her Ph.D in 2004 from the University of Warwick, United Kingdom in optical communication engineering. She has served UTM since 1998 as an academic and administrative staff. Her main research interests are optical communication system and network, optoelectronic design, and engineering management. Her research output has been translated into a number of publications (H-index-17) and IPR including a high-end reference book, 'Optical Wireless Communication: IR Connectivity' published by Taylor and Francis, 49 book chapters and monographs, over 200 refereed research papers, 8 patents granted, 36 patent filings and holds 31 UTM copyrights. She is Senior Member of IEEE and member of Editorial Board of few refereed international journals. She has been appointed as Guest Professor at Osaka Prefecture University and Tokai University, Japan in 2011 and 2014, respectively. She can be contacted at email: sevia@utm.my.

Shahrin Md Ayob 🆔 is a lecturer in Faculty of Electrical Engineering, Universiti Teknologi Malaysia (UTM) since 2009. He received the B.E.E., M.E.E., and Ph.D. degrees from the Universiti Teknologi Malaysia (UTM), Kuala Lumpur, in 2000, 2003 and 2009, respectively. He is currently with the Department of Energy Conversion, Faculty of Electrical Engineering, UTM, Skudai, Malaysia. His current interest of research is on the application of artificial intelligence on power converters. He can be contacted at email: e-shahrin@utm.my.